JMEPEG (2010) 19:171–176
DOI: 10.1007/s11665-009-9392-z

1059-9495/$19.00

Comparison Between Structures and Properties of ABS Nanocomposites Derived from Two Different Kinds of OMT

Yibing Cai, Fenglin Huang, Xin Xia, Qufu Wei, Xutao Tong, Anfang Wei, and Weidong Gao

(Submitted May 19, 2008; in revised form February 7, 2009)

In the present work, the hexadecyl triphenyl phosphonium bromide (P16) and cetyl pyridium chloride (CPC) were used to modify montmorillonite (MMT) based on the structural characteristic of the engineering thermoplastic acrylonitrile-butadiene-styrene copolymer (ABS) and the principle of "like dissolves like", and then used to prepare the ABS/organic-modified montmorillonite (OMT) nanocomposites by melt-intercalation method. The influences of two different kinds of OMT on the structures and properties of the ABS nanocomposites were characterized by x-ray diffraction (XRD), transmission electron microscopy (TEM), high-resolution electron microscopy (HREM), thermogravimetric analyses (TGA), Cone calorimetry and dynamic mechanical analyses (DMA), respectively. The increased basal spacing showed that ABS intercalated into the gallery of the OMT. The morphology indicated that the OMT dispersed well in the ABS resin and the intercalated structure for ABS/OMT-P16 nanocomposites and intercalated-exfoliated structure for ABS/OMT-CPC nanocomposites were respectively formed. The TGA results revealed that onset temperature of thermal degradation and charred residue at 700 °C of the ABS nanocomposites was remarkably enhanced compared to the pure ABS. It was also found from the Cone calorimetry tests that the peak of heat release rate (PHRR) decreased significantly, contributing to the reduced flammability. The DMA measurements indicated that the loading of silicate clays improved the storage modulus of the ABS resin. The partial exfoliation of the OMT-CPC within ABS nanocomposites was advantageous to increasing thermal stability properties, decreasing flammability properties, and improving mechanical properties.

Keywords acrylonitrile-butadiene-styrene copolymer (ABS), engineering thermoplastic, flammability, mechanical properties, nanocomposites, organic-modified montmorillonite (OMT), thermal stability

1. Introduction

Acrylonitrile-butadiene-styrene copolymer (ABS) has been widely used as an important engineering thermoplastics owing to its desirable properties, which include good mechanical properties, chemical resistance, and easy processing characteristics. However, one of the main drawbacks of the ABS resin is its lower thermal stability and inherent flammability. Therefore, there is a need to increase its thermal stability and flame retardant properties (Ref 1-3). Polymer/clay nanocomposites are believed to be a new promising approach in fire retardancy. The dispersion of these ultra-thin (1 nm) ultra-high surface-area clay layers (usually <10 wt.%) within a polymer matrix led to nanocomposites exhibiting markedly improved physicochemical properties, better dimensional and thermal stabilities, improved gas barrier properties and reduced flammability, compared with pure polymers or conventional microcomposites (Ref 4, 5).

The preparation of polymer nanocomposites may be accomplished either by in situ polymerization or by melt blending. Jang et al. (Ref 6) studied ABS/montmorillonite (MMT) nanocomposites prepared by direct intercalation through one-step emulsion polymerization. The onset temperature of decomposition shifted to the higher temperature region as much as 40-50 °C when the MMT content reached 33.3 wt.%, though the direct intercalation was not accompanied by delamination of the clay layers. Ying and Fung (Ref 7) reported that composites prepared by an in situ sol-gel process had greatly increased tensile strength, glass transition temperature (T_g), and thermal stability because of the existence of the covalent bond between the ABS chains and the silica network, which increased the compatibility between the organic and inorganic phases. Choi et al. (Ref 8) synthesized the ABS/clay nanocomposites by using two clays (sodium montmorillonite, laponite). Both colloidal stability and mechanical properties of the nanocomposites depended on aspect ratios of clays. Wang et al. (Ref 9) prepared intercalated-exfoliated structure of ABS nanocomposites by melt blending ABS and organic-modified clay. Wilkie and co-workers (Ref 10-17) had also done significant works to enhance the thermal stability and compatibility of the modified clay by the generation of novel surfactants, including a stibonium-modified clay (Ref 10), a tropylium cation modified clay (Ref 11), and various oligomerically modified clays (Ref 12-17).

Yibing Cai, Fenglin Huang, Qufu Wei, Xutao Tong, Anfang Wei, and **Weidong Gao**, Key Laboratory of Eco-Textiles, Ministry of Education, Jiangnan University, Wuxi 214122 Jiangsu, People's Republic of China; and **Xin Xia**, Xinjiang University, Wulumuqi 830046 Xinjiang, People's Republic of China. Contact e-mail: yibingcai@jiangnan.edu.cn.

Based on the above literature summaries, it can be found that two major factors, compatibility and thermal stability, must be considered in order to get nanocomposites by melt blending. To improve the interactions between the clay and polymer, the clay must be modified. The usual treatment is that the cations between the clay layers are replaced by alkylammonium or phosphonium cation through ion-exchange method. The modified clay must be sufficiently compatible with the polymer and must be thermally stable under the processing conditions. In the present work, based on the structure characteristic of the ABS resin and the principle of "like dissolves like", the hexadecyl triphenyl phosphonium bromide (P16) and cetyl pyridium chloride (CPC) were chosen to prepare the higher thermal stability organic-modified montmorillonite (OMT), and further used to prepare the ABS/OMT nanocomposites by the melt-intercalation method. The influences of two different OMT on the structures and properties of the nanocomposites were investigated and then compared with the pure ABS resin. The loading of the OMT remarkably increased thermal stability, decreased flammability, and improved mechanical properties of the ABS nanocomposites.

2. Experimental

2.1 Materials

The acrylonitrile-butadiene-styrene copolymer (ABS, PA-757K) was supplied as pellets by the Qimei Plastic Limited Company (Zhenjiang, China). The original purified sodium montmorillonite (MMT, with a cation exchange capacity (CEC) of 97 meq/100 g) was kindly provided by Fenghong Clay Chemical Limited Company, Zhejiang. The P16 and CPC were purchased from Shanghai Chemicals Company. The structures of engineering thermoplastic ABS copolymer, P16 and CPC are presented in Scheme 1.

2.2 Fabrication of OMT

The OMT were prepared by cation-exchange reaction of Na^+ with P16 or CPC. In total, 10.0 g of MMT and 5.40 g of P16 were added to 400 mL distilled water in 500 mL flask. The mixtures were stirred vigorously for 2 h at 80 °C before the P16-exchanged silicates were collected by filtration. The solids were subsequently washed with hot distilled water until the supernatant liquid was tested by a 0.1 mol/L $AgNO_3$ solution without yielding sedimentation. The product was then dried in vacuum and ground into powder to get the OMT-P16. The preparation procedure for OMT-CPC was similar to that for the OMT-P16. Then, 10.0 g of MMT and 3.44 g of CPC were added to 400 mL distilled water in 500 mL flask and stirred vigorously for 5 h at 80 °C. The solids were washed, dried, and ground into powder to obtain the OMT-CPC.

2.3 Preparation of ABS/OMT Nanocomposites

The OMT and ABS resin were dried under vacuum at 80 °C for overnight before use. The ABS resin was melt-mixed with OMT in a twin-roll mill (XK-160, Jiangsu, China) for 10 min. The temperature and the roll speed of the mill were set at 180 °C and 100 rpm, respectively. The prepared ABS nanocomposites were compressed and molded into sheets (1 and 3 mm thickness). The mass fraction of the OMT to ABS was 4 wt.%, and was referred to as ABS/OMT-P16 and ABS/OMT-CPC nanocomposites, respectively.

2.4 Characterization

The Fourier transform infrared (FT-IR) spectra were recorded on a Nicolet MAGNA-IR 750 spectrometer by the standard KBr disk method in the range of 350-4000 cm^{-1} with a resolution of 4 cm^{-1}.

X-ray diffraction (XRD) patterns were obtained on the 1 mm thick films using a Japanese Rigaku D/Max-Ra rotating anode x-ray diffractometer equipped with a Cu-Kα tube and Ni filter (λ = 0.1542 nm).

To investigate the dispersion of the clay layers within the nanocomposites, the photographs were taken on a Hitachi model H-800 transmission electron microscopy (TEM) and high-resolution electron microscopy (HREM, JEOL 2010) with an accelerating voltage of 200 kV. The TEM and HREM specimens were cut at room temperature using an ultramicrotome (Ultracut-1, UK) with a diamond knife from an epoxy block with the films of the nanocomposites embedded. Thin specimens, 50-80 nm, were collected in a trough filled with water and placed on 200 mesh copper grids.

Thermogravimetric analyses (TGA) were carried out by using a TGA50H thermo-analyzer instrument from 25 to

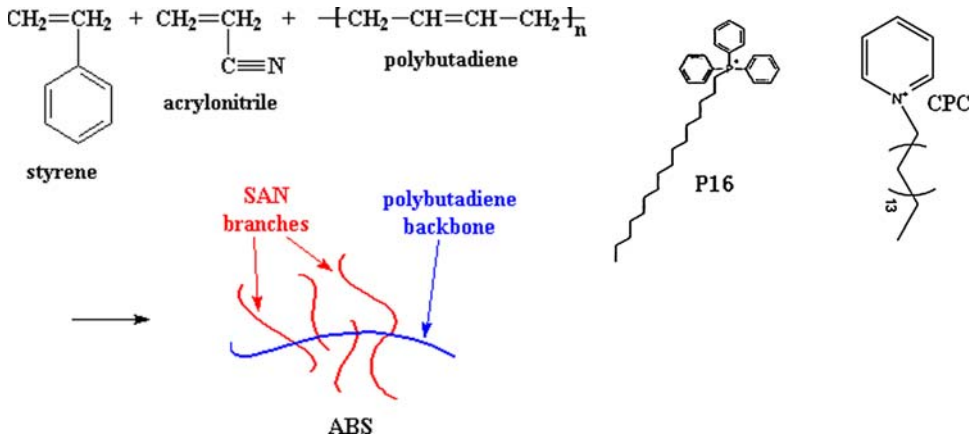

Scheme 1 Structures of ABS copolymer, P16 and CPC

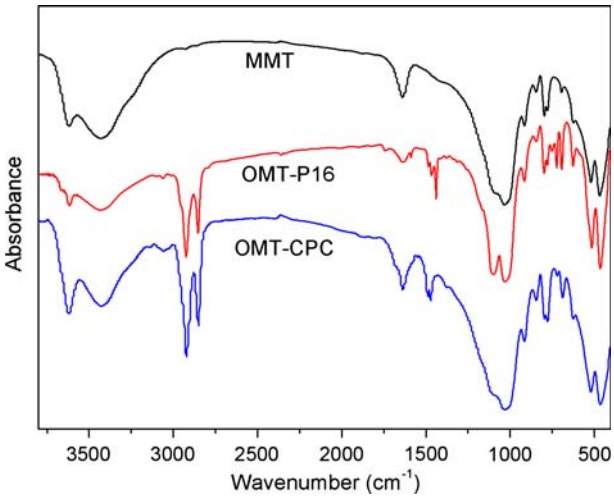

Fig. 1 FT-IR spectra of the MMT, OMT-P16, and OMT-CPC

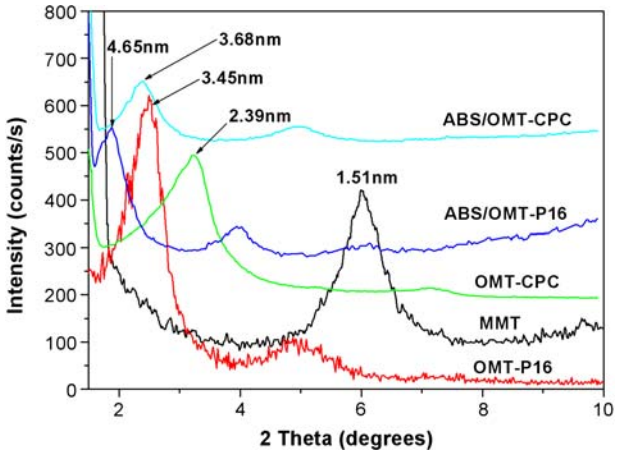

Fig. 2 XRD response curves of the MMT, OMT-P16, OMT-CPC, and the corresponding ABS/OMT nanocomposites

700 °C with a linear heating rate of 10 °C/min under nitrogen flow. The nitrogen flow was 25 mL/min. Samples were measured in a sealed alumina pan with a mass of about 10 mg.

Flammability property was characterized by Cone calorimetry. The signals from the Cone calorimetry were recorded and analyzed by a computer system. All samples ($100 \times 100 \times 3$ mm^3) were examined in a Stanton Redcroft Cone calorimetry according to ISO 5660 under a heat flux of 35 kW/m^2. Exhaust flow rate was 24 L/s and the spark was continued until the sample ignited. The typical results from Cone calorimetry were reproducible to within ±10%.

The dynamic mechanical analyses of materials were carried out by using a Tritec 2000B Dynamic Mechanical Analyser from 30 to 160 °C with a heating rate that raised the temperature by 5 °C/min. The deformation and frequency were 0.04% and 1 Hz, respectively. The samples (dimension $15 \times 9 \times 1$ mm) were molded in 180 °C for 10 min under 5 MPa of pressure.

3. Results and Discussion

3.1 Structure and Morphology

The FTIR spectra of the MMT, OMT-P16, and OMT-CPC are shown in Fig. 1. The characteristic bands of MMT were 3620, 1032, 512, and 460 cm^{-1}, corresponding to the stretching vibration of O-H, the stretching vibration of Si-O-Si, the stretching vibration of Al-O, and the Si-O bending vibration of MMT, respectively. The characteristic peaks at around 3055, 1438, 1112 cm^{-1} and 2923, 2840 cm^{-1} were the stretching and bending vibrations of PPh_3, and the stretching vibration of the hexadecane from P16, respectively. The peaks at 2915, 2850 cm^{-1} and those around 1480 cm^{-1} were assigned to the characteristic bands of the symmetric and asymmetric stretching vibrations and bending vibration of methylene groups from CPC respectively. The results confirmed that the cationic surfactants (P16 and CPC) had tethered into the interlayers of the silicate clay.

The XRD patterns of the MMT, OMT-P16, OMT-CPC and the corresponding ABS/OMT nanocomposites are shown in Fig. 2. The peaks corresponded to the (001) plane reflection of the silicate clays. It was observed from XRD curves that the diffraction peaks of silicate clay after organic modification shifted to a lower angle. The corresponding average basal spacing of the MMT increased from 1.51 to 3.45 nm (OMT-P16) and 2.39 nm (OMT-CPC), respectively. The increased spacing confirmed that the cationic surfactants intercalated into the galleries of the MMT. It can be found from XRD curves that the basal spacing of the silicate clays increased from 3.45 nm of the OMT-P16 to 4.65 nm and remained the second diffraction peak, which indicated the formation of an intercalated structure. For the ABS/OMT-CPC nanocomposites, it shows that the basal spacing increased to around 3.68 nm from 2.39 nm of the OMT-CPC. The XRD results indicated that the ABS resin intercalated into the silicate clay layers.

To further investigate the dispersion of silicate clay layers within the ABS resin, the morphology of the ABS nanocomposites characterized by TEM and HREM is presented in Fig. 3 and 4, respectively. The silicate clay layers looked well dispersed throughout the ABS resin and some larger intercalated tactoids (multiplayer particles) were visible, as indicated in Fig. 3. The TEM images indicated that there was a greater interaction between the silicate clays and ABS resin. The differences in the morphology of the two nanocomposites characterized by HREM are shown in Fig. 4. It was observed from Fig. 4(a) that the intercalated structure with a significant number of tactoids consisted of several clay layers in the ABS/OMT-P16 nanocomposites. Although the phenyl groups deriving from P16 were similar to the ABS molecular chains, there were 3 phenyl groups which were not there in the same plane. The spatial barrier effects among the 3 phenyl groups may hinder the better dispersion of silicate clays within the ABS resin. Hence the alkyl groups of the P16 may be more dominant to the dispersion of silicate clays within the ABS resin and formed the intercalated structure. The HREM image in Fig. 4(b) shows that single clay platelets were observed, besides multilayers tactoids. This meant that the silicate clay layers were partially exfoliated within the ABS resin and an intercalated-exfoliated mixed structure was formed, due to the heteroaromatic ring groups of CPC molecular chains being similar to the phenyl structure of the ABS chains. The similar molecular structures contributed to the partial exfoliation of the OMT-CPC, which may be expected to possess more favorable interactions between the OMT-CPC and the ABS chains.

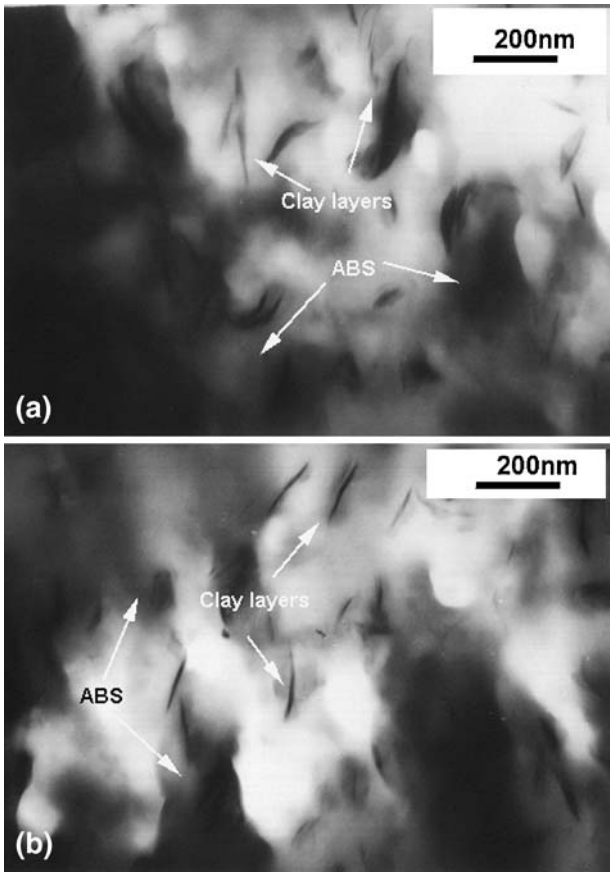

Fig. 3 TEM images of (a) ABS/OMT-P16 nanocomposites and (b) ABS/OMT-CPC nanocomposites

3.2 Thermal Stability Properties

Thermal stability is an important property for which the nanocomposites morphology played an important role. The thermal stability properties of the ABS nanocomposites were discussed and compared with those of pure ABS. The TGA curves are shown in Fig. 5. The onset degradation temperatures (defined as the loss temperature at 5 wt.%) increased from 364.5 °C for pure ABS resin to 365.2 °C for ABS/OMT-P16 nanocomposites and 374.3 °C for ABS/OMT-CPC nanocomposites, respectively. The thermal decomposition of the ABS nanocomposites shifted toward a higher temperature range compared to the pure ABS. And the yield of charred residue at 700 °C for the ABS/OMT-P16 and ABS/OMT-CPC nanocomposites was respectively increased from 3.01 wt.% for the pure ABS to 4.76 and 6.21 wt.%. After about 480 °C, the TGA curves became flat and mainly the inorganic residue (i.e., Al_2O_3, MgO, SiO_2) remained. The increased charred residue contributed to the improved thermal stability properties of the ABS nanocomposites. This was attributed to the nanosize silicate clay layers which could presumably facilitate the reassembly of lamellas to form three-dimensional char, which might occur on the surface of the nanocomposites and create a physical protective barrier. Meanwhile, the silicate clay layers could act as a superior insulator and mass-transport barrier to the volatile products generated during the thermal decomposition for increasing the thermal stability (Ref 18).

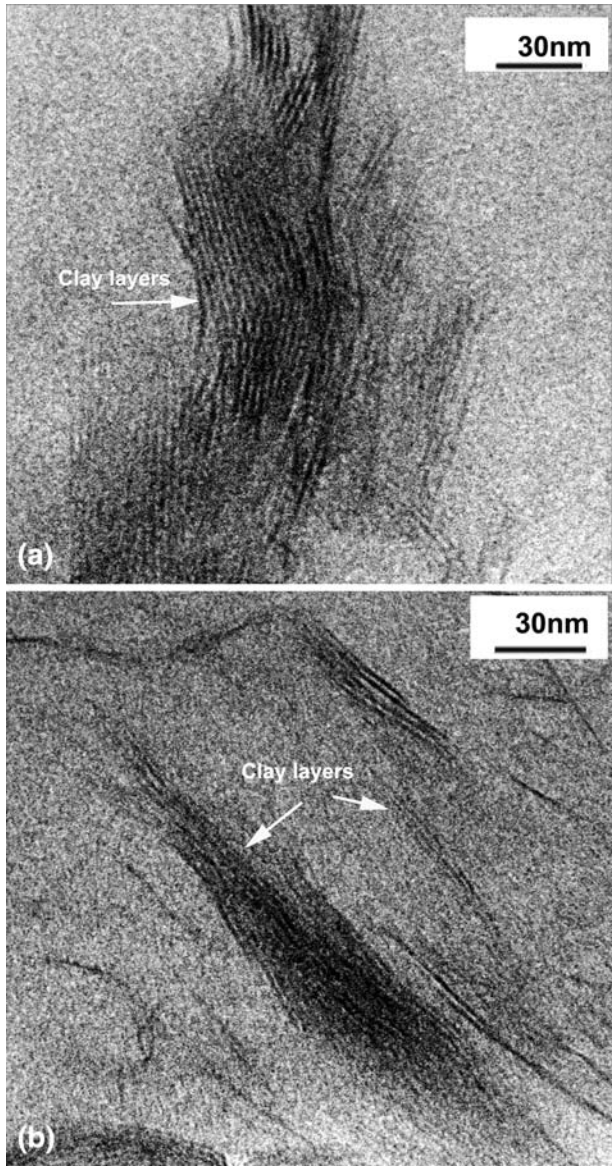

Fig. 4 HREM images of (a) ABS/OMT-P16 nanocomposites and (b) ABS/OMT-CPC nanocomposites

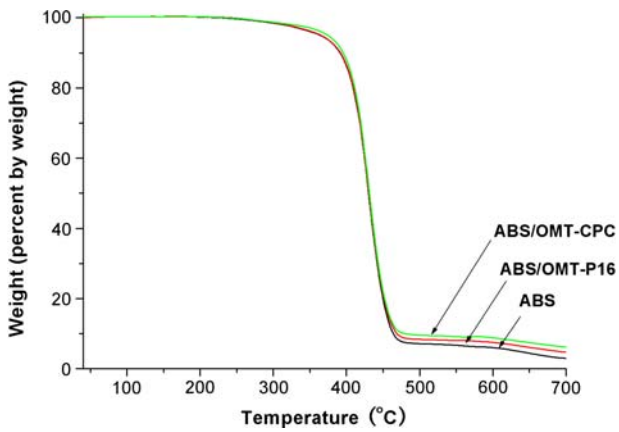

Fig. 5 Thermogravimetric analyses curves of the pure ABS and ABS/OMT nanocomposites

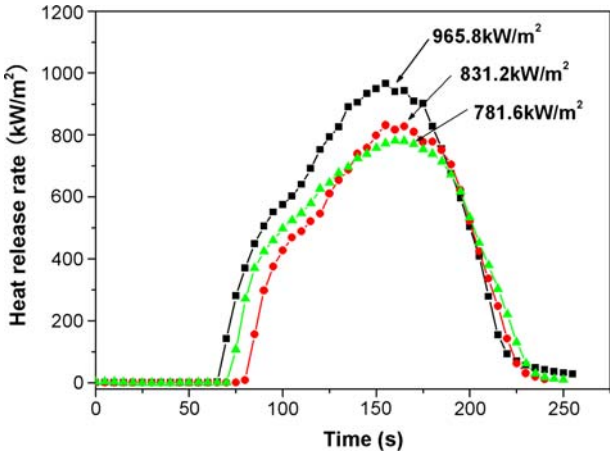

Fig. 6 The curves of heat release rate responses to time for the pure ABS and ABS/OMT nanocomposites

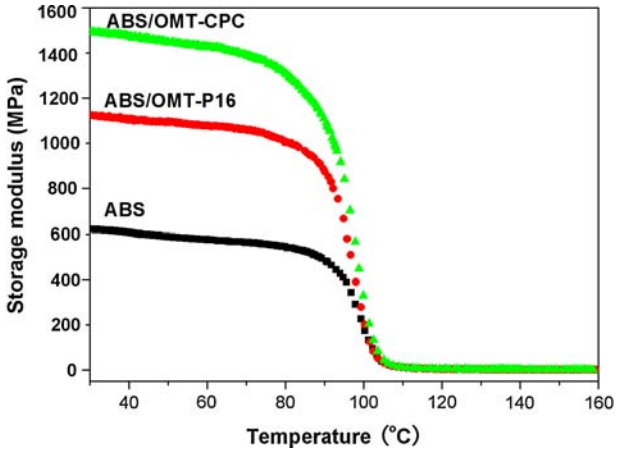

Fig. 7 The curves of storage modulus responses to temperature for the pure ABS and ABS/OMT nanocomposites

It was interesting to find from TGA curves that the thermal stability properties of the ABS/OMT-CPC nanocomposites were slightly higher than those of the ABS/OMT-P16 nanocomposites. The onset thermal degradation temperature and charred residue at 700 °C of ABS/OMT-CPC nanocomposites increased respectively about 9 °C and 1.5 wt.% compared to ABS/OMT-P16 nanocomposites. The reasons may be that the cationic surfactant in the OMT-CPC contained heteroaromatic ring groups, which were similar to the phenyl groups of ABS chains in structure, contributing to better dispersion of silicate clays. The well dispersion was propitious to the improved thermal properties.

3.3 Flammability Properties

The Cone calorimetry is one of the most effective bench scale methods for investigating the combustion properties of polymer materials. The peak of heat release rate (PHRR) had been found to be one of the most important parameters to evaluate fire safety (Ref 18, 19). The flammability properties of the ABS nanocomposites were characterized by Cone calorimetry in the present study. The HRR curves of the pure ABS and its nanocomposites at a heat flux of 35 kW/m^2 are illustrated in Fig. 6. The PHRR of the ABS/OMT-P16 nanocomposites and ABS/OMT-CPC nanocomposites decreased respectively from 965.8 kW/m^2 for pure ABS to 831.2 and 781.6 kW/m^2. The PHRR decrease of the ABS nanocomposites was due to the barrier effects of silicate clay layers. It was also found that the PHRR of ABS/OMT-CPC nanocomposites was slightly lower than that of ABS/OMT-P16 nanocomposites, due to the exfoliation and well dispersion of silicate clays, as indicated in Fig. 4. The decreased tendency of PHRR also corresponded with the increased tendency of thermal stability, as characterized by TGA analyses. The loading of silicate clays led to the decreases of the PHRR, contributing to the reduced flammability performances.

3.4 Mechanical Properties

Dynamic mechanical analyses (DMA) measure the response of a given material to a cyclic deformation (usually tension or three-point flexion type deformation) as a function of the temperature. The storage modulus is one of the important parameters of the DMA measurements, corresponding to the elastic response to the deformation. The dynamic mechanical behaviors of the ABS nanocomposites were also investigated in the present work. The storage modulus curves of the pure ABS and ABS nanocomposites are shown in Fig. 7. It was observed from Fig. 7 that the storage modulus at 25 °C of the pure ABS and ABS nanocomposites were respectively 6.222×10^2 MPa (pure ABS), 1.130×10^3 MPa (ABS/OMT-P16 nanocomposites), and 1.502×10^3 MPa (ABS/OMT-CPC nanocomposites). The incorporation and better dispersion of silicate clays increased remarkably the storage modulus of the ABS nanocomposites. It can be also found that the storage modulus of the ABS/OMT-CPC nanocomposites was slighter higher than that of the ABS/OMT-P16 nanocomposites. It was believed that intercalated-exfoliated mixed structure for ABS/OMT-CPC nanocomposites played an important role, as indicated in Fig. 4(b). It was well known that the mechanical properties of the nanocomposites were enhanced relative to those of the pure polymers and that delaminated nanocomposites were enhanced relative to intercalated nanocomposites (Ref 20).

4. Summary

Based on structure characteristic of engineering thermoplastic ABS copolymer and the principle "like dissolves like", the P16 and CPC were chosen to modify the MMT and then used to prepare the ABS nanocomposites by melt-mixing method. The structures of the OMT characterized by FT-IR spectra and XRD indicated that the cationic surfactants intercalated into the interlayers of silicate clay. The structures and properties of the ABS nanocomposites were characterized by XRD, TEM, HREM, TGA, Cone calorimetry, and DMA, respectively. The results indicated that an intercalated structure and intercalated-exfoliated mixed structure were respectively formed for ABS/OMT-P16 nanocomposites and ABS/OMT-CPC nanocomposites. The onset degradation temperature and charred residue of the ABS nanocomposites had remarkably increased compared to the pure ABS. It was also found from the Cone calorimetry tests that the PHRR decreased significantly, contributing to the reduced flammability properties. The DMA measurements showed that the silicate clays improved notably the storage modulus of the ABS resin, attributed to the increased mechanical

properties of nanocomposites. The results also indicated the influences of structure and morphology on properties of ABS nanocomposites. The partial exfoliation of the silicate clays was advantageous to increasing thermal stability properties, decreasing flammability properties, and improving mechanical properties of nanocomposites.

Acknowledgments

The work was financially supported by the Program for New Century Excellent Talents in University (No. NCET-06-0485), the Research Fund for the Doctoral Program of Higher Education of China (No. 200802951011), and the Natural Science Initial Research Fund of Jiangnan University (No. 2008LYY002).

References

1. S.R. Owen and J.F. Harper, Mechanical, Microscopical and Fire Retardant Studies of ABS Polymers, *Polym. Degrad. Stab.*, 1999, **64**, p 449–455
2. K. Zheng, L. Chen, Y. Li, and P. Cui, Preparation and Thermal Properties of Silica-Graft Acrylonitrile-Butadiene-Styrene Nanocomposites, *Polym. Eng. Sci.*, 2004, **44**, p 1077–1082
3. Y.B. Cai, Y. Hu, L. Song, S.Y. Xuan, Y. Zhang, Z.Y. Chen, and W.C. Fan, Catalyzing Carbonization Function of Ferric Chloride Based on Acrylonitrile-Butadiene-Styrene Copolymer/Organophilic Montmorillonite Nanocomposites, *Polym. Degrad. Stab.*, 2007, **92**, p 490–496
4. A. Usuki, Y. Kojima, M. Kawasumi, A. Okada, T. Kurauchi, and O. Kamigatio, Synthesis of Nylon 6-Clay Hybrid, *J. Mater. Res.*, 1993, **8**, p 1179–1184
5. R.A. Vaia, H. Ishii, and E.P. Giannelis, Synthesis and Properties of 2-Dimensional Nanostructure by Direct Intercalation of Polymer Melts in Layered Silicates, *Chem. Mater.*, 1993, **5**, p 1694–1696
6. L.W. Jang, C.M. Kang, and D.C. Lee, A New Hybrid Nanocomposite Prepared by Emulsion Copolymerization of ABS in the Presence of Clay, *J. Polym. Sci. B: Polym. Phys.*, 2001, **39**, p 719–727
7. G.H. Ying and J.L. Fung, Organic-Inorganic Composite Materials from Acrylonitrile-Butadiene-Styrene Copolymers and Silica Through an In Situ Sol-Gel Process, *J. Appl. Polym. Sci.*, 2000, **75**, p 275–283
8. Y.S. Choi, M.Z. Xu, and I.J. Chung, Synthesis of Exfoliated Acrylonitrile-Butadiene-Styrene Copolymer (ABS) Clay Nanocomposites: Role of Clay as a Colloidal Stabilizer, *Polymer*, 2005, **46**, p 531–538
9. S.F. Wang, Y. Hu, L. Song, Z.Z. Wang, Z.Y. Chen, and W.C. Fan, Preparation and Thermal Properties of ABS/Montmorillonite Nanocomposite, *Polym. Degrad. Stab.*, 2002, **77**, p 423–426
10. D. Wang and C.A. Wilkie, A Stibonium-Modified Clay and its Polystyrene Nanocomposite, *Polym. Degrad. Stab.*, 2003, **82**, p 309–315
11. J. Zhang and C.A. Wilkie, A Carbocation Substituted Clay and its Styrene Nanocomposite, *Polym. Degrad. Stab.*, 2004, **83**, p 301–307
12. X.X. Zheng, D.D. Jiang, D.Y. Wang, and C.A. Wilkie, Flammability of Styrenic Polymer Clay Nanocomposites Based on a Methyl Methacrylate Oligomerically-Modified Clay, *Polym. Degrad. Stab.*, 2006, **91**, p 289–297
13. J.G. Zhang, D.D. Jiang, and C.A. Wilkie, Fire Properties of Styrenic Polymer-Clay Nanocomposites Based on an Oligomerically-Modified Clay, *Polym. Degrad. Stab.*, 2006, **91**, p 358–366
14. J.G. Zhang, D.D. Jiang, D.Y. Wang, and C.A. Wilkie, Mechanical and Fire Properties of Styrenic Polymer Nanocomposites Based on an Oligomerically-Modified Clay, *Polym. Adv. Technol.*, 2005, **16**, p 800–806
15. S. Su, D.D. Jiang, and C.A. Wilkie, Polybutadiene-Modified Clay and its Nanocomposites, *Polym. Degrad. Stab.*, 2004, **84**, p 279–288
16. S. Su, D.D. Jiang, and C.A. Wilkie, Novel Polymerically-Modified Clays Permit the Preparation of Intercalated and Exfoliated Nanocomposites of Styrene and its Copolymers by Melt Blending, *Polym. Degrad. Stab.*, 2004, **83**, p 333–346
17. S. Su, D.D. Jiang, and C.A. Wilkie, Poly(methyl methacrylate) Polypropylene and Polyethylene Nanocomposite Formation by Melt Blending Using Novel Polymerically-Modified Clays, *Polym. Degrad. Stab.*, 2004, **83**, p 321–331
18. J.W. Gilman, C.L. Jakson, A.B. Morgan, R.H. Harris, E. Manias, E.P. Giannelis, M. Wuthenow, D. Hilton, and S.H. Philips, Flammability Properties of Polymer-Layered-Silicate Nanocomposites: Polypropylene and Polystyrene Nanocomposites, *Chem. Mater.*, 2000, **12**, p 1866–1873
19. J.W. Gilman, Flammability and Thermal Stability Studies of Polymer Layered-Silicate (Clay) Nanocomposites, *Appl. Clay Sci.*, 1999, **15**, p 31–49
20. M. Alexander and P. Dubois, Polymer-Layered Silicate Nanocomposites: Preparation, Properties and Uses of a New Class of Materials, *Mater. Sci. Eng.*, 2000, **28**, p 1–63